Biosensors and Bioelectronics 43 (2013) 446–452

Contents lists available at SciVerse ScienceDirect

Biosensors and Bioelectronics

journal homepage: www.elsevier.com/locate/bios

Self-assembly of quantum dots/denatured BSA-oligonucleotides bioconjugate and its application on aptameric gold nanoparticles-based biosensor for the determination of rHuEPO-α

Jiefang Sun, Lei Guo*, Hua Xu, Jijun Tang, Jianwei Xie*

Beijing Institute of Pharmacology and Toxicology, No. 27, Taiping Road, Beijing 100850, China

ARTICLE INFO

Article history:
Received 25 October 2012
Received in revised form
13 December 2012
Accepted 14 December 2012
Available online 3 January 2013

Keywords:
QDs
AuNPs
rHuEPO-α
Ligand
Aptamer
Detection

ABSTRACT

In this paper, denatured bovine serum albumin (dBSA) has been developed as a useful scaffold for appending multiple oligonucleotides (ODNs), and the resulted novel dBSA-ODNs covalent hybrid can be self-assembled to the surface of CdTe quantum dots (QDs) *via* complexation with unoccupied coordination metal sites on QDs' surface. The formed QDs/dBSA-ODNs bioconjugate could keep a long-term stability in aqueous solution while maintaining its fluorescence quantum yield and spectral properties. Furthermore, the QDs/dBSA-ODNs also can be readily hybridized with an anti-rHuEPO-α aptamers linked AuNPs (Apt-AuNPs) to form a fluorescent resonance energy transfer-based nano-biosensing system for highly sensitive and selective detection of rHuEPO-α protein lowered to 53.6 pM in a rapid, simple manner.

1. Introduction

As a kind of promising nanomaterial which possesses unique electronic and optical properties (Alivisatos, 1996; Gao et al., 2005), quantum dots (QDs) have been established as targeting, imaging or diagnostic tools in the biomedical fields over the past decade (Medintz et al., 2005; Michalet et al., 2005; Wu et al., 2003). Before serving to certain purpose, the bare QDs need to be derived with chemical or biological modules (Edgar et al., 2006) to generate suitable surface structure or functionality. The applications of QDs are greatly hinged on the researches of the manipulation of their surface chemistry for constructing the biocompatible, water-soluble, monodispersed and compact nano-bioconjugates, while their long-term stability and optical properties should still be maintained or improved.

Several approaches, such as bi-functional covalent linkage, ligand-exchange, and self-assembly have been attempted to generate QDs bioconjugates. For example, the common way to prepare QDs bioconjugates is a direct cross-linking approach *via* bi-functional linker agents. Although simple in concept, multiple purification steps are included in this approach and it is not easy to be reproduced. Besides, the use of linker agents are always susceptible to make QDs form aggregation so as to lead fluorescence quenching (Clapp et al., 2006; Medintz et al., 2005; Shen et al., 2009). Another rapid and simple way is ligand-exchange using thiol terminated functional biomolecules (Pinaud et al., 2004), but both excessive amounts of bio-ligands and multiple purification steps are needed. Further, considering that thiol bond is easy to be photo-oxidized, the ligands attached to thiol can then fall off from the surface of the QDs and precipitation occurs. These limitations accelerate researchers to find more favorable QDs surface modification strategies with a diversity of characteristics and good colloidal stability as well.

Over recent years, self-assembly has been evolved to be an interesting alternative for the construction of hybrid nanocomposites (Whitesides and Grzybowski, 2002). Direct deposition of suitable (macro) molecules on the QDs is an attractive conjugation approach. It is often rapid, has high binding/affinity constants, and also avoid many problems occurred from covalent chemistry and subsequent purification steps. A typical self-assembly strategy to functionalize the surface of QDs based on metal-histidine interaction between QDs and proteins, peptides and DNA has been recently introduced (Medintz et al., 2007; Medintz and Mattoussi, 2009; Sapsford et al., 2007). In such a strategy, the reactive peptide linker $(His)_6$ is conjugated to a variety of biomolecules and enable their rapid self-assembly onto QDs with high-affinity. The features of this strategy are, it simplifies both the assembling chemistry and purification procedures, furthermore, it has higher controllability on the association sites and the orientations of the immobilized biological moieties attached per QDs.

* Corresponding authors. Tel./fax: +86 10 6822 5893.
E-mail addresses: guolei@bmi.ac.cn, sunjf2001@163.com (L. Guo), xiejw@nic.bmi.ac.cn (J. Xie).

0956-5663/$ - see front matter © 2013 Elsevier B.V. All rights reserved.
http://dx.doi.org/10.1016/j.bios.2012.12.040

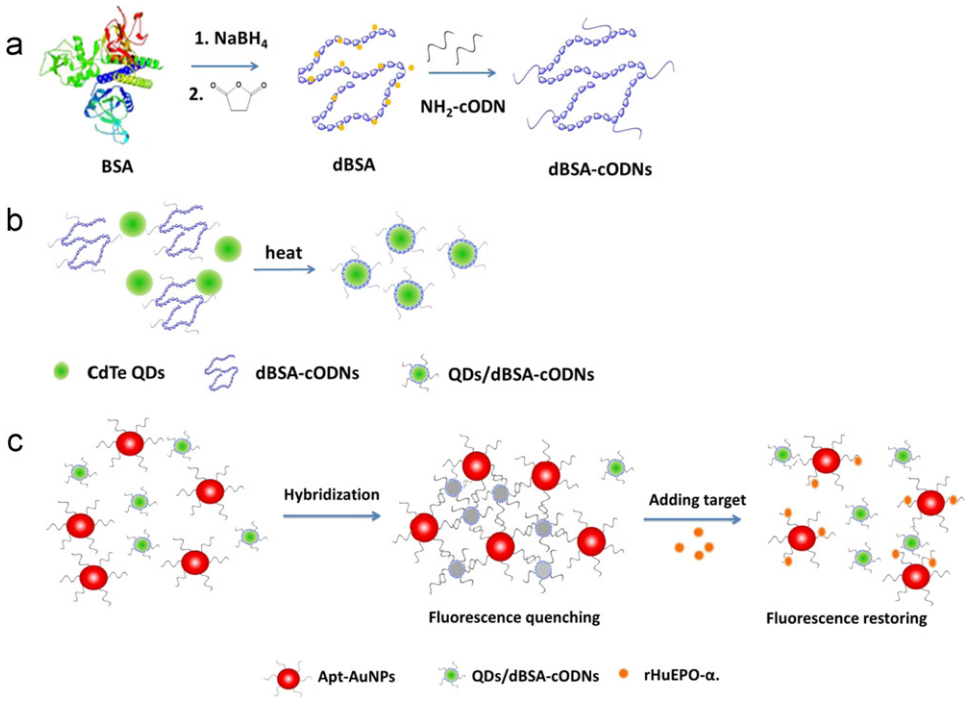

Scheme 1. (a) The formation of dBSA-cODNs hybrid. (b) The self-assembly of dBSA-cODNs hybrid on CdTe QDs and (c) The QDs/dBSA-cODNs and Apt-AuNPs assemblies for rHuEPO-α detection.

In this paper, a simple, direct, and reproducible method for fabricating CdTe QDs and single stranded oligonucleotides (ODNs) conjugation is proposed. Firstly, a denatured bovine serum albumin (dBSA)-ODNs covalent hybrid is synthesized and characterized. This ligand exhibits high affinity toward CdTe QDs and can be readily self-assembly on QDs surface. The capping layer of dBSA-ODNs can maintain QDs optical properties and long term stability in aqueous solution, at the same time eliminating nonspecific adsorption of QDs to other proteins.

To further demonstrate the applications of this QDs/dBSA-ODNs nano-bioconjugate, we introduce aptamers for erythropoietin (EPO) in virtue of specific aptamer-EPO protein interaction. Aptamers are single stranded DNA ligands isolated from combinatorial oligonucleotide libraries by *in vitro* selection (Tuerk and Gold, 1990). They can recognize a variety of chemical and biological molecules with high affinity and selectivity, and thus regarded as a kind of novel affinity recognition elements for biosensing and diagnostic fields (Nutiu and Li, 2005). EPO is an important endogenously hematopoietic growth factor, which can promote the proliferation and differentiation of erythroid progenitor cells and maintain the red blood cell mass at an optimum level. Recombinant human erythropoietin (rHuEPO) has been produced in 1990 by biological recombinant techniques as an effective biopharmaceutical, and widely applied in clinic for anemia treatment associated with renal disease and cancer (Choi et al., 1996). Recently, our research group has successfully generated a series of DNA aptamers of highly specific for rHuEPO-α (Zhang et al., 2010).

In this paper, we devise a simple fluorescence turn-on sensing strategy for rHuEPO-α based on proposed QDs/dBSA-cODNs. In such a strategy, the anti-rHuEPO-α aptamers (807–35nt) modified AuNPs (Apt-AuNPs) and their complementary ODNs sequences (cODNs) functionalized QDs/dBSA-cODNs can be hybridized to an ideal signal transduction module for the detection of rHuEPO-α according to a competing binding principle. In the presence of rHuEPO-α, they could specifically bind to aptamers on the surface of AuNPs, and the base pairs formed between QDs/dBSA-cODNs and Apt-AuNPs become loosen, then the fluorescence resonance energy transfer (FRET) between QDs donors and AuNPs acceptors are blocked. Finally, the fluorescence restored (Scheme 1). This nano-biosensing method offers high selectivity and sensitivity for the detection of rHuEPO-α in physiological buffer at tens of pM level.

2. Materials and methods

2.1. Chemicals and instruments

rHuEPO-α (3.89 mg/mL, purity > 98.5%) was kindly provided by SCIPROGEN Bio-pharmaceutical Co. (Shenzhen, China) and diluted to the standard solution of 1 μM containing 0.1% BSA. 3-Mercaptopropionic acid (MPA, +99%), tellurium (Te, 200 mesh, 99.8%), $NaBH_4$ (98%), $CdCl_2 \cdot 2.5H_2O$, (99.99%), BSA (98%), 1-ethyl-3-(3-dimethylaminopropyl) carbodiimide (EDC) and sulfo-N-hydroxysuccinimide (sulfo-NHS, 97.0%) were purchased from Sigma Aldrich Inc. (St. Louis, MO, USA). Other reagents were of analytical grade or even better and purchased from SinoPharm Chemical Reagent Co. Ltd (Beijing, China). The 807–35 nt aptamer (5′–SH-A_9 GAT TGA AAG GTC TGT TTT TGG GGT TGG TTT GGG TCA A-3′, here A_9 indicates the poly(dA) linker), and its cODN sequences (5′ NH_2-AAA AAA TTG ACC C-3′) were obtained from Sangon Biological Engineering Technology & Co. Ltd. (Shanghai, China) and used as received. The physiological buffer was consisted of 20 mM Tris–HCl, 140 mM NaCl, 5 mM $MgCl_2$ and 5 mM KCl (pH 7.4). BCA protein assay kit was the product of Vigorous Biotechnology Beijing Co. Ltd (Beijing, China). Sterilized ultrapure water was produced through a Milli-Q Ultrapure Water System (Millipore, Billerica, MA, USA).

Nicolet 6700 Fourier transform infrared spectrometer (FT-IR, Thermo Scientific, USA) was used to characterize the dBSA-cODNs hybrid and QDs/dBSA-cODNs nanoparticles. Fluorescence spectra were collected using a LS-55 fluorescence spectrometer (Perkin Elmer, Waltham, MA, USA). The excitation was set at 400 nm with

a recording emission range of 500–600 nm. Both excitation and emission slit were set at 5 nm. The sizes of CdTe QDs were verified by H-7650 transmission electron microscope (TEM, Hitachi High-Technologies Co., Tokyo, Japan). The plasma absorption of AuNPs was measured in a Cary 300 double-beam UV–vis spectrophotometer (Varian, Palo Alto, CA, USA).

2.2. Synthesis and characterization of 3-mercaptopropionic acid stabilized CdTe QDs

MPA stabilized hydrophilic CdTe QDs was prepared by using $CdCl_2 \cdot 2.5H_2O$ and NaHTe as precursors based on a previously reported method (Gao et al., 1998) and the QDs was collected after refluxing 2 h. These QDs were purified twice with ultrapure water through filtration in Microcon 10 kD spin filters (Millipore, Billerica, MA, USA) at 5000 rpm to remove unreacted compounds, and then redissolved in ultrapure water. The concentration of purified QDs solution was determined according to Beer's law using an extinction coefficient of $1.65 \times 10^5\ M^{-1}\ cm^{-1}$ (Yu et al., 2003).

2.3. Synthesis of AuNPs and aptamer modified AuNPs

The spherical AuNPs of 12 nm diameter were prepared through citrate-mediated reduction of $HAuCl_4$ (Storhoff et al., 1998). Aqueous $HAuCl_4$ (1 mM, 200 mL) was heated to a vigorous boiling state while stirring in a round-bottom flask with a reflux condenser. Trisodium citrate (38.8 mM, 20 mL) was added rapidly to the boiling solution. It could be found that the solution turned to an intense dark violet firstly then quickly changed to red. The solution was refluxed for an additional 15 min at boiling status, and then cooled to room temperature with continuous stirring for another 15 min. To purify the AuNPs, the solution was centrifuged for 20 min at 14,000 rpm and decantated by supernatants, and then the resulting AuNPs were resuspended in ultrapure water. The shape and size of AuNPs were characterized by TEM and shown as monodisperse, spherical particles with an average diameter of 12 nm. The plasma absorption peak was measured by UV–vis spectroscopy. The concentration of the AuNPs could calculate as 15 nM according to Beer's law using an extinction coefficient of $2.4 \times 10^8\ M^{-1}\ cm^{-1}$ at 520 nm for the 12 nm AuNPs (Hill et al., 2009).

The 5′-thiol-modified anti-rHuEPO-α aptamers were directly linked onto the surface of AuNPs through Au–S affinity. Aqueous aptamers (100 μM, 20 μL) were added into the AuNPs solution (15 nM, 1.0 mL). According to Ref. (Hill et al., 2009), the conjugates were salted in 0.3 M NaCl, and then purified *via* centrifugation and resuspension in sterile ultrapure water. Finally, the aptamer modified AuNPs (Apt-AuNPs) were equilibrated with 0.1% BSA for 4 h at room temperature before use. This BSA-blocked Apt-AuNPs can prevent nonspecific binding with interference proteins (Huang et al., 2005).

To determine the number of aptamers on each AuNP, dithiothreitol (DTT, 0.1 M, 100 μL) was added the solution of Apt-AuNPs (12 nM, 100 μL) to cleave the Au–S bond and release all conjugated aptamer from the AuNPs. After overnight incubation at 50 °C, the dissociated aptamers were separated from AuNPs by centrifugation, and the absorbance intensity at 260 nm of supernatant containing displace aptamers were measured, an average number of 40 aptamers per particle was determined.

2.4. Preparation of dBSA-cODNs hybrid

dBSA was prepared by treating BSA with $NaBH_4$ according to Ref. (Wang et al., 2006). The resulted dBSA were further modified by succinic anhydride to convert the primary amine groups of dBSA to carboxyl groups according to Ref. (Kuo et al., 2008). The reaction mixture was purified through filtration in Microcon 10 kD spin filters at 5000 rpm to remove excessive components. The cODN (5′ NH_2-AAA AAA TTG ACC C-3′) was then linked to dBSA through EDC/sulfo-NHS reaction. In detail, EDC (5.0 mg) and sulfo-NHS (3.0 mg) were firstly mixed with dBSA solution (48 μM, 1.0 mL) in 10 mM 2-(N-morpholino) ethanesulfonic acid (MES) buffer at pH 4.5. The mixture was reacted for 20 min under room temperature, and after that purified *via* centrifugated ultrafiltration and resuspended in $NaHCO_3$ buffer at pH 8.5 (10 mM, 1.0 mL).

To the prepared dBSA solution, various amounts of NH_2-cODN were added and the ratio of dBSA and cODN were set as 1:3, 1:4 and 1:5, respectively, these mixtures were incubated at 4 °C for 48 h. The resulting dBSA-cODNs mixtures were purified *via* centrifugated ultrafiltration, and then resuspended in 1.0 mL sterile ultrapure water and stored at 4 °C. The final concentration of the dBSA-cODNs was determined as $4.5 \times 10^{-5}\ mol\ L^{-1}$ using BCA assay kit. To confirm the chemical binding between NH_2-cODN and dBSA, the product was run in 12% non-denatured polyacrylamide gel electrophoresis (PAGE) at $22\ V\ cm^{-1}$ for 1 h. The gel was then stained in ethidium bromide (EB) and imaged by DIGI Doc-IT bioimaging system (UVP Co., USA).

2.5. Self-assembly of dBSA-cODNs hybrid on CdTe QDs

The purified CdTe QDs solution was mixed with the dBSA-cODNs hybrid solution with a molar ratio of QD:dBSA-cODN at 1:1. The mixture was heated at 90 °C for 20 min to facilitate the full self-assembly of dBSA-cODNs to the CdTe QDs. After that, the solution was stored at 4 °C for another 2 days. The reaction mixture was filtered by Microcon 100 kD spin filters at 5000 rpm to remove the unreacted QDs and other impurities. The final product was redissolved in sterile ultrapure water and stored at 4 °C. To confirm the assembly between QDs and dBSA-cODNs, the product was run in 2% agarose gel electrophoresis for 30 min.

2.6. Preparation of rHuEPO-α sensor using Apt-AuNPs and QDs/dBSA-cODNs

The selection buffer consisted of 20 mM Tris–HCl, 140 mM NaCl, 5 mM $MgCl_2$ and 5 mM KCl (pH 7.4) was chosen to provide favorable binding between rHuEPO-α and aptamer 807–35 nt (Zhang et al., 2010). Typically, the Apt-AuNPs (50 μL, 15 nM) and the QDs/dBSA-cODNs (5 μL, 0.35 μM) were mixed in the selection buffer. The mixture was heated to 90 °C for 3 min, then maintained at 4 °C for 6 h. Such treatment resulted in the hybridization of Apt-AuNPs and QDs/dBSA-cODNs, as evidenced by fluorescence quench phenomenon due to FRET effect.

2.7. Optimizing the hybridization ratio between QDs/dBSA-cODNs and Apt-AuNPs

Different volumes of the Apt-AuNPs (15 nM) and the QDs/dBSA-cODNs (5 μL, 0.35 μM) were mixed in the selection buffer to 400 μL, making the mixing ratio at 1:1, 2:1, 5:1 and 10:1, respectively. After hybridization process, 10 μL of rHuEPO-α were added into these solutions, and kept them at room temperature for 5 h. Finally, the solutions were transferred into a quartz cuvette to collect the fluorescence spectra.

2.8. Competitive assay

For both the Apt-AuNPs and QDs/dBSA-cODNs at a fixed concentration, aliquots of rHuEPO-α (10 μL) with different amounts were added to form the sensing system, and further

kept at room temperature for 5 h. After that the fluorescence of such a sensing system was measured as a function of the rHuEPO-α concentration.

Different interfering proteins including HSA, IgG, transferrin, globin, lysozyme and cytochrome C were used to examine the specificity of the method. Each of the interfering proteins (1 μM) were added to the sensing system in the presence of rHuEPO-α (40 nM) in the selection buffer. After being kept at room temperature for 5 h, the solution was transferred into a quartz cuvette to collect the fluorescence spectra.

3. Results and discussions

To successfully apply inorganic nanomaterials in biosystems, it is of great importance to tune their surface properties and construct suitable bio-functionalized one. BSA is a potentially excellent candidate to cover and functionalize the surface of nanomaterials, since it contains a wide range of accessibly reactive groups offered by simply modifying the terminus or other constituent residues for conjugation to other molecules (Ma et al., 2008; Peelle et al., 2005). It was previously reported that BSA had been used as a capping/stabilizing agent for various metal and semiconductor nanoparticles (Bakshi et al., 2009; Shang et al., 2007; Wu et al., 2010).

On such a basis, we use denatured albumins capping agent, *i.e.*, dBSA, as scaffold for covalently appending multiple cODNs as the recognition motifs. The full dBSA-cODNs hybrid can readily self-assembly onto the unoccupied coordination metal sites on the QDs surface according to metal-affinity driven interaction (Scheme 1). Comparing with BSA, dBSA have more flexible linear structure instead of original complex spatial conformation, so it makes dBSA much feasible to be covalently linked with higher reaction reproducibility.

3.1. Characterization of the dBSA-cODNs hybrid

Firstly, cODNs are covalently linked to the dBSA scaffold through amide formation using carbodiimide-mediated cross-linking chemistry (Scheme 1a). There are primary bands specific for dBSA in the FT-IR spectra (see Fig. S1 in Supplementary data), including the amide I band at 1649 cm^{-1} and the amide II band at 1534 cm^{-1}. Comparing with dBSA, the dBSA-cODNs have a particularly sharp band at 1150 cm^{-1} corresponding to the bones of phosphorous group, which indicates the presence of cODN.

Non-denatured PAGE is adopted to confirm the covalent bound between cODNs and dBSA. A typical PAGE gram is shown in Supplementary data Fig. S2, in which the prepared hybrids at different dBSA/cODNs ratios are applied as the samples and dBSA itself as the control band. After being stained with EB, only the dBSA-cODNs could be stained by this DNA-intercalating dye (lanes 2–4) compared to the dark band of dBSA (lane 1). The same gel is then re-stained with Commassie Blue to show the existence of protein, and the dBSA-cODNs at different ratios have the same mobility as that of unmodified dBSA. Both results suggest the successful linkage is formed between dBSA and cODNs.

3.2. Self-assembly of dBSA-cODNs hybrid on the surface of QDs

Colloidal QDs have a large fraction of their atoms placed on their surfaces; they can be easily capped with biofunctional ligands due to the presence of defected surface states contributed from dangling bonds and incomplete passivation. Previous researches showed that a gentle thermal treatment of dBSA and ODNs prior to assemble onto the nanoparticles induces drastic conformational relaxation of the dBSA or ODNs molecules into an extended, linear conformation (Barhoumi et.al, 2008; Bakshi et al., 2009). Under heating process, unfolded protonated amino acids of dBSA-cODNs are expected to be in a better position to effectively access to the CdTe QDs surface and interact with them, which might easily deposit relatively greater amounts of dBSA-cODNs on the QDs surface. Besides, heating process could facilitate the ligand anchor on the surface of QD and efficiently removed many surface defects and dangling bonds (Byrne et al., 2006; Wang et al., 2006). The dBSA-cODNs ligand contains two distinct functional domains, dBSA is the scaffold responsible for metal-affinity-driven self-assembly to CdTe QDs, and the cODNs can easily perform their specific binding towards their complementary sequences (Scheme 1b).

Firstly, we characterized the QDs/dBSA-cODNs hybrid in gel electrophoresis. As shown in Fig. 1, the electrophoretic mobility of QDs/dBSA-cODNs with different dBSA/cODN ratios had distinctive difference (lanes 2–4) from the bare CdTe QDs in 2% agarose gel (control, lane 1). It is owing to the increased molecular weight of dBSA-cODNs upon the formation of QDs/dBSA-cODNs. This result illuminates that the dBSA-cODNs could assemble on the surface of QDs. But the resolution of 2% agarose gel is limited; it could not distinguish the electrophoretic motilities between QDs/dBSA-cODNs with different amount of cODNs per dBSA.

We also employed FT-IR spectroscopy to investigate the conjugation behavior of QDs/dBSA-cODNs. FT-IR spectra of the pure dBSA-cODNs, QDs/dBSA-cODNs with different cODNs per dBSA are shown in Fig. 2. It is worthwhile mentioned that the signal at 1451 cm^{-1} in the dBSA-cODNs ligand, which correspond to the symmetrical stretching vibration of C=O units in dBSA, is decreased in the QDs/dBSA-cODNs at the ratio of 1:3 (b), 1:4 (c), thus indicating that these dBSA-cODNs ligands possibly anchor to the QDs through these C=O. Besides, the typical FT-IR bands of the dBSA-cODNs, amide II at 1541 cm^{-1}, amide I groups at 1650 cm^{-1} for dBSA, 1050 cm^{-1} for the cODN, match with those of QDs conjugates (b and c) very well. However, it is found that the unmasked band of C=O of QDs/dBSA-cODNs with dBSA/cODN ratio at 1:5 in 1451 cm^{-1} (d).

Combining Figs. 1 and 2, we can address the maximum number of cODNs per dBSA when self-assembly occurred on the surface of QDs. Because cODN are big electronegative molecules, they could cause steric and electrostatic hindrance when

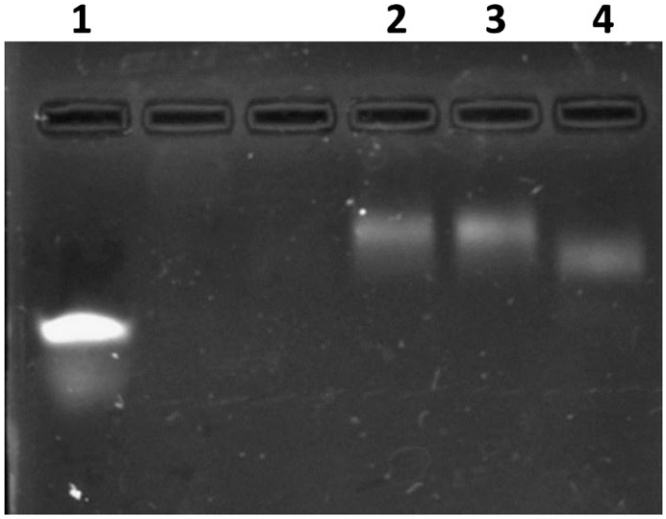

Fig. 1. 2% agarose gel electrophoresis of CdTe QDs before and after capped with dBSA-cODNs. Lane 1 represented the bare CdTe QDs, and lanes 2–4 represented dBSA-cODNs hybrids self-assembled on CdTe QDs at the dBSA/cODN ratio of 1:3, 1:4 or 1:5, respectively.

accessing to dBSA (pI 4.6, also shows negative in physiological buffer) and further electronegative QDs. The result demonstrates that, when the number of cODNs per dBSA beyond four, the ligand possibly fails to self-assemble on CdTe QDs, which could be verified by the much weaker band of dBSA/cODN ratio at 1:5 (lane 4, Fig. 1), and the unmasked band of C=O units band in 1451 cm^{-1} (Fig. 2).

In Fig. 3, the TEM image reveals that the QDs with or without dBSA-cODNs are all well-dispersed and the diameters of QDs/dBSA-cODNs (nearly 8 nm) are larger than the bare CdTe QDs (2–4 nm). Comparing the fluorescent spectra of bare QDs and QDs/dBSA-cODNs (see Fig. S3 in Supplementary data), the latter gain a 21% enhancement of fluorescence intensity but no change of band peak position and band width, indicating that the core of CdTe QDs have kept its original size after being capped with dBSA-cODNs. Theoretically, the enhancement of QDs photoluminescence intensity is explained by the decrease in non-radioactive transitions or their speeds, which can be achieved by the elimination or mask the defects on QDs surface. It is considered that dBSA take a positive effect on fluorescence intensity by capping on the surface of QDs, and dBSA with multiple binding sites provide further enhanced coordination interaction to the surface of CdTe QDs. Therefore, the chemical stability of the QDs/dBSA-cODNs is effectively improved. In Fig. S3, it is shown that the fluorescence intensity of the bare CdTe QDs decreases by more than 80%, however, after modification of QDs/dBSA-cODNs quenches 30% within 50 days, both of them were purified and dispersed in aqueous solution at room temperature. As previous literature reported, the purified QDs are more easily being aggregated and result in fluorescence quench, because the oxidization of capping agent with the help of light (Derfus et al., 2004). The addition of surface capping agent, here is dBSA, typically increase the quantum yield and stability of QDs, by limiting surface oxidation.

Over 6 months storage in refrigerator at 4 °C, no visible aggregate appeared in the as-synthesized QDs/dBSA-cODNs solution and the fluorescence intensity decreased by nearly 80%. However, the purified CdTe QDs have aggregate and show no fluorescence.

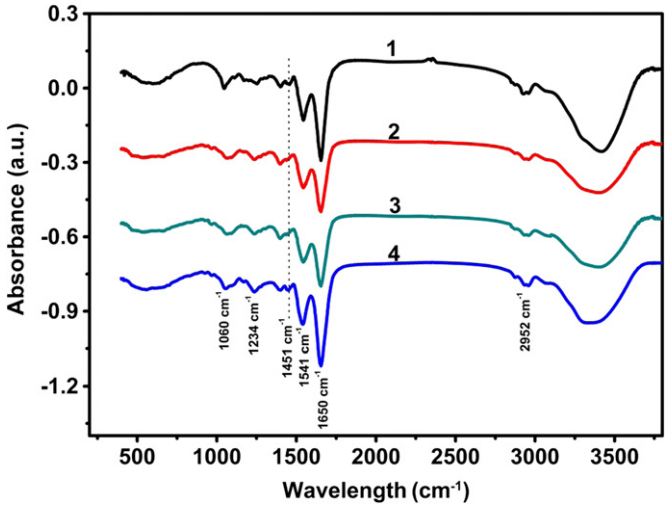

Fig. 2. FT-IR spectra of dBSA-cODNs (a), and QDs/dBSA-cODNs at dBSA/cODN ratio of 1:3 (b), 1:4 (c) or 1:5 (d), respectively.

3.3. CdTe QDs/Apt-AuNPs nano-biosensor for rHuEPO-α

Benefited from the hybridization ability of cODN, and the enhanced fluorescence and stability of such water-soluble QDs/dBSA-cODNs, it is ready to design a fluorescence "signal-on" sensing strategy to demonstrate the application of this bioconjugation (Scheme 1c). QDs is a favorable donor in the FRET system due to its distinct optical characteristics (Quach et al., 2011; Oh et al., 2005), while AuNPs is an efficient photoluminescence quencher because of its high extinction coefficient (the extinction coefficient of $2.4 \times 10^8\ M^{-1}\ cm^{-1}$ at 520 nm for the 12 nm AuNPs). A broad absorption spectrum of AuNPs is overlapped with the emission wavelength of QDs donors, which then compose perfect FRET pair. We employed the Apt-AuNPs as an effective proximal quencher through hybridization with QDs/dBSA-cODNs according to our proposed procedures.

The sequence of cODN adopted in the QDs/dBSA-cODNs has 6 bases complementary to the 807–35 nt aptamer, such a base-pair length is suitable for cODN at good hybridization, and readily departure status when compete with target protein (Maxwell et al., 2002). We prepared Apt-AuNPs through citrate capped AuNPs with a 5′-SH rHuEPO-α aptamer. The surface plasmon band of this Apt-AuNPs is slightly shifted from 520 nm (bare AuNPs) to 522 nm, which is mainly attributed to the change of the surface charge status and charge transfer upon aptameric modification.

We then generated a nanobiosensor for the sensitive and selective determination of rHuEPO-α. Firstly, the hybridization between Apt-AuNPs and CdTe QDs/dBSA-cODNs induces the fluorescence quenching of the QDs by the proximity of AuNPs. In the presence of the rHuEPO-α target molecule, the specific binding force between aptamer and target protein makes the aptamer fold into suitable three-dimensional shape to fit rHuEPO-

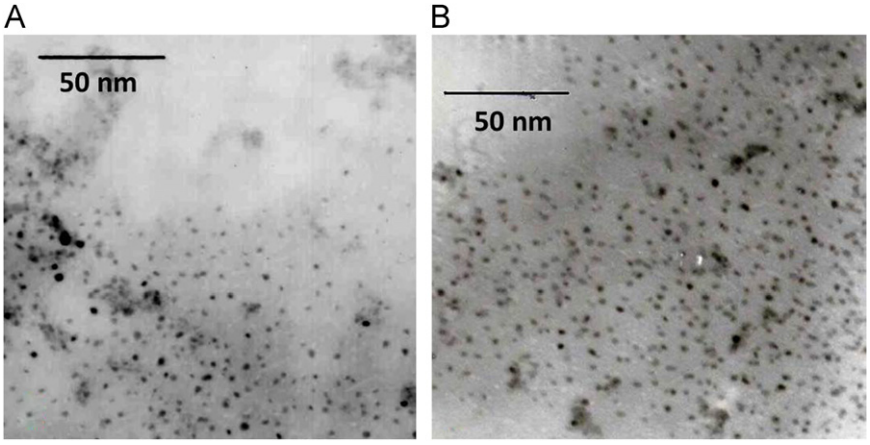

Fig. 3. Typical TEM images of the bare CdTe QDs (A) and CdTe QDs/dBSA-cODNs (B).

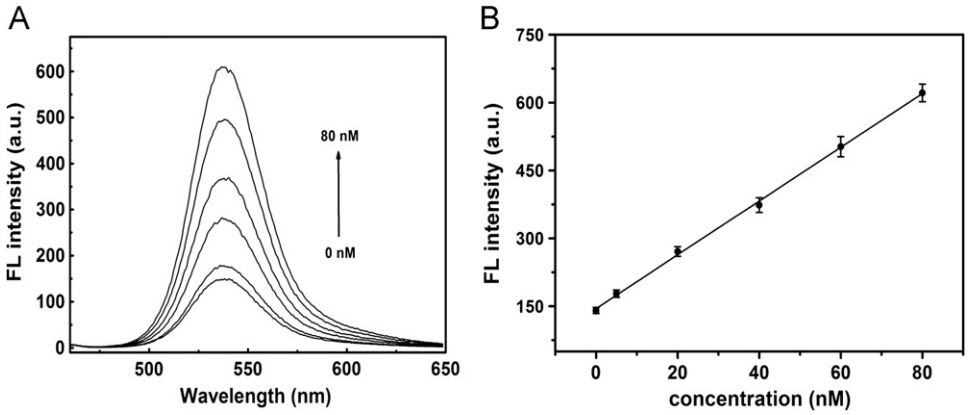

Fig. 4. (A) Fluorescence "signal-on" measurement of rHuEPO-α. (B) The linear relationship between relative fluorescence (FL) intensity ($F-F_0$, where F and F_0 are the fluorescence intensity obtained with the rHuEPO-α and the blank, respectively). Each point reflects the average of four independent experiments. Error bars indicate standard deviations. The buffer is consisted of 20 mM Tris–HCl, 140 mM NaCl, 5 mM $MgCl_2$ and 5 mM KCl at pH 7.4, other conditions see Section 2.

α to disrupt the base-pairing between the QDs/dBSA-cODNs and the Apt-AuNPs, finally causes the QDs/dBSA-cODNs being released from the surface of Apt-AuNPs with a restore in the fluorescence intensity. This molecular recognition event can thus be effectively converted into a measurable signal.

Upon the hybridization between Apt-AuNPs and QDs/dBSA-cODNs, the fluorescence quench extends and further sensitivity for rHuEPO-α is dependent on the hybridization ratio between QDs/dBSA-cODNs and Apt-AuNPs. As shown in Fig. S4, when certain concentrations of QDs/dBSA-cODNs hybridize with ever-increasing amount of Apt-AuNPs, the fluorescence quenching efficiency shows drastic decrease. It is demonstrated that in such a system, adding more Apt-AuNPs could make more efficient hybridization to QDs and reach a relatively lower background, but it also provide more binding aptamer site for the rHuEPO-α in AuNPs which do not participate in breaking the base pairs between QDs/dBSA-cODNs and Apt-AuNPs. The target molecule rHuEPO-α could specifically bind to its aptamers in AuNPs whenever they hybridized with QDs/dBSA-cODNs or not, so the presence of excess Apt-AuNPs has an unfavorable effect for signal recovery. Finally, we chose the Apt-AuNPs and QDs/dBSA-cODNs at hybridization ratio of 2:1 as the optimal condition.

We further evaluated the performance of this nanosensing system for the detection of rHuEPO-α. As shown in Fig. 4A, the peak intensity is increased with continuous addition of rHuEPO-α. Fig. 4B represents a linear relationship between the relative FL intensity and the concentration of rHuEPO-α (relative $FL=144.1+5.97C_{rHuEPO-\alpha}$, $R^2=0.999$). The linear range for rHuEPO-α is from 5 to 60 nM. We then calculated the LOD as 53.6 pM according to the equation of $LOD=3SD_{blank}/k$ (where k represents the slope of linear curve, the repeated number of blank is 10). Comparing with our previously developed method using AuNPs as the acceptor and fluorescent dye as the donor (Sun et al., 2011), the sensitivity of current method is improved one order of magnitude.

To address the selectivity of this nano-biosensing system, we also examined various common co-existed interfering proteins. It is found that the addition of 25-fold common proteins do not produce a significant increase in fluorescent signal (see Fig. S5 in Supplementary data). These results are consistent with the selective binding ability of aptamer for its target.

4. Conclusions

To conclude, we report a simple and practical self-assembly approach for fabricating the QDs/dBSA-ODNs nanobioconjugate, whose optical properties maintain well and the stability is being improved. This strategy enables us to fulfill at least two purposes in one simple step, dBSA-ODNs ligand passivates the underlying QDs surfaces and provides multiple appending ODNs equipped on QDs. In such of the nanobioconjuate material, dBSA functions as the scaffold for covalently appending multiple ODNs and metal-affinity-driven capping layer on CdTe QDs. The QDs/dBSA-ODNs nanobioconjugate has been further applied to a sensitive protein detection platform based on the specific interaction between the aptamer and rHuEPO-α, and a fluorescent system is established by monitoring the FRET between QDs/dBSA-cODNs and Apt-AuNPs. Such a method shows high sensitivity and good selectivity in virtue of using aptamer as recognition module, and offers great potential for a simple, rapid biomonitoring of this important protein in biological samples.

Acknowledgments

This project was supported by the National Natural Science Foundation of China (Nos. 21175152 and 81001262).

Appendix A. Supplementary information

Supplementary data associated with this article can be found in the online version at http://dx.doi.org/10.1016/j.bios.2012.12.040.

References

Alivisatos, A.P., 1996. Science 271, 933–937.
Bakshi, M.S., Thakur, P., Kaur, G., Kaur, H., Banipal, T.S., Possmayer, F., Petersen, N.O., 2009. Advanced Functional Materials 19, 1–8.
Barhoumi, A., Zhang, D.M., Tam, F., Halas, N.J., 2008. Journal of the American Chemical Society 130, 5523–5529.
Byrne, S.J., Corr, S.A., Rakovich, T.Y., Gunko, Y.K., Rakovich, Y.P., Donegan, J.F., Mitchell, S., Volkov, Y., 2006. Journal of Material Chemistry 16, 2896–2902.
Choi, D., Kim, M., Park, J., 1996. Journal of Chromatography B 687, 189–199.
Clapp, A.R., Goldman, E.R., Mattoussi, H., 2006. Nature Protocols 1, 1258–1266.
Derfus, A.M., Chan, W.C.W., Bhatia, S.N., 2004. Nano Letters 4, 11–14.
Edgar, R., McKinstry, M., Hwang, J., Oppenheim, A.B., Fekete, R.A., Giulian, G., Merril, C., Nagashima, K., Adhya, S., 2006. Proceedings of the National Academy of Sciences of the United States of America 103, 4841–4845.
Gao, M., Rogach, A.L., Kornowski, A., Kirstein, S., Eychmuller, A., Mohwald, H., Weller, H., 1998. Journal of Physical Chemistry B 102, 8360–8363.
Gao, X., Yang, L., Petros, J.A., Marshall, F.F., Simons, J.W., Nie, S.M., 2005. Current Opinion in Biotechnology 16, 63–72.
Hill, H.D., Millstone, J.E., Banholzer, M.J., Mirkin, C.A, 2009. ACS Nano 3, 418–424.

Huang, C.C., Huang, Y.F., Cao, Z., Tan, W., Chang, H.T., 2005. Analytical Chemistry 77, 5735–5741.
Kuo, Y.C., Wang, Q., Ruengruglikit, C., Yu, H., Huang, Q., 2008. Journal of Physical Chemistry C 112, 4818–4824.
Ma, N., Sargent, E.H., Kelley, S.O., 2008. Journal of Materials Chemistry 18, 954–964.
Maxwell, D.J., Taylor, J.R., Nie, S., 2002. Journal of the American Chemical Society 124, 9606–9612.
Medintz, A.L., Berti, L., Pons, T., Grimes, A.F., English, D.S., Alessandrini, A., Facci, P., Mattoussi, H., 2007. Nano Letters 7, 1741–1748.
Medintz, I.L., Uyeda, H.T., Goldman, E.R., Mattoussi, H., 2005. Nature Materials 4, 435–446.
Medintz, I.L., Mattoussi, H., 2009. Physical Chemistry Chemical Physics 11, 17–45.
Michalet, X., Pinaud, F.F., Bentolila, L.A., Tsay, J.M., Doose, S., Li, J.J., Sundaresan, G., Wu, A.M., Gambhir, S.S., Weiss, S., 2005. Science 307, 538–544.
Nutiu, R., Li, Y.F., 2005. Angewandte Chemie-International Edition 44, 1061–1065.
Oh, E., Hong, M.Y., Lee, D., Nam, S.H., Yoo, H.C., Kim, H.S., 2005. Journal of the American Chemical Society 127, 3270–3271.
Peelle, B.R., Krauland, E.M., Wittrup, K.D., Belcher, A.M., 2005. Langmuir 21, 6929–6933.
Pinaud, F., King, D., Moore, H.P., Weiss, S., 2004. Journal of the American Chemical Society 126, 6115–6123.
Quach, D., Crivat, G., Tarr, M.A., Rosenzweig, Z., 2011. Journal of the American Chemical Society 133, 2028–2030.
Sapsford, K.E., Pons, T., Medintz, I.L., Higashiya, S., Brunel, F.M., Dawson, P.E., Mattoussi, H., 2007. Journal of Physical Chemistry C 111, 11528–11538.
Shang, L., Wang, Y., Jiang, J., Dong, S., 2007. Langmuir 23, 2714–2721.
Shen, H.Y., Jawaid, A.M., Snee, P.T., 2009. ACS Nano 3, 915–923.
Storhoff, J.J., Elghanian, R., Mucic, R.C., Mirkin, C.A., Letsinger, R.L., 1998. Journal of the American Chemical Society 120, 1959–1964.
Sun, J.F., Guo, A.T., Zhang, Z.Y., Guo, L., Xie, J.X., 2011. Sensors 11, 10490–10501.
Tuerk, C., Gold, L., 1990. Science 249, 505–510.
Wang, Q., Kuo, Y., Wang, Y., Shin, G., Ruengruglikit, C., Huang, Q., 2006. Journal of Physical Chemistry B 110, 16860–16866.
Whitesides, G.M., Grzybowski, B., 2002. Science 295, 2418–2421.
Wu, X.Y., Liu, H.J., Liu, J.Q., Haley, K.N., Treadway, J.A., Larson, J.P., Ge, N.F., Peale, F., Bruchez, M.P., 2003. Nature Biotechnology 21, 41–46.
Wu, Y., Chakrabortty, S., Gropeanu, R.A., Wilhelmi, J., Xu, Y., Er, K.S., Kuan, S.L., Koynov, K., Chan, Y.T., Weil, T, 2010. Journal of the American Chemical Society 132, 5012–5014.
Yu, W.W., Qu, L.H., Guo, W.Z., Peng, X.G., 2003. Chemistry of Materials 15, 2854–2860.
Zhang, Z., Guo, L., Guo, A.T., Xu, H., Tang, J.J., Guo, X.J., Xie, J.W., 2010. Bioorganic & Medicinal Chemistry 18, 8016–8025.